

Cartoon Hallucinations Detection: Pose-aware In Context Visual Learning

Bumsoo Kim^{1*}, Wonseop Shin^{1*}, Kyuchul Lee², Sanghyun Seo^{1†}

¹Chung-Ang University, South Korea

²VIVE STUDIOS, South Korea

{bumsookim, wonseop218, sanghyun}@cau.ac.kr, lk880425@vivestudios.com

Abstract

Large-scale Text-to-Image (TTI) models have become a common approach for generating training data in various generative fields. However, visual hallucinations, which contain perceptually critical defects, remain a concern, especially in non-photorealistic styles like cartoon characters. We propose a novel visual hallucination detection system for cartoon character images generated by TTI models. Our approach leverages pose-aware in-context visual learning (PA-ICVL) with Vision-Language Models (VLMs), utilizing both RGB images and pose information. By incorporating pose guidance from a fine-tuned pose estimator, we enable VLMs to make more accurate decisions. Experimental results demonstrate significant improvements in identifying visual hallucinations compared to baseline methods relying solely on RGB images. This research advances TTI models by mitigating visual hallucinations, expanding their potential in non-photorealistic domains.

1. Introduction

Leveraging machine-generated images with large Text-to-Image (TTI) models [26–29] has become a common technique in image and video generation [6, 37]. Recently, beyond TTI generation, complex multi-modal approaches combining Visual Language Models (VLMs) [1, 2, 21, 38] upon LLMs with Large Language Models (LLMs) [31, 41] are being utilized together with TTI to obtain more compelling and imaginative images. This is achieved by using reference images [39] or human-level image captioning [13] for training and inference [6, 37], thanks to the appealing output generated according to textual prompts.

However, TTI and VLMs [19] often suffer from the visual hallucination problem, similar to the hallucination issue in language models under LLMs [14, 34]. In image and video formats, a phenomenon called "visual hallucination"

occurs when images appear clear at first glance but show major inaccuracies upon closer examination. This means that even though the images seem correct initially, they actually contain errors that become obvious when you look more closely. These inaccuracies compromise the models' reliability and trustworthiness, posing challenges for network training and the broader adoption of large-scale generative models.

Recent progress in the field of in-context visual learning has shown promising results in addressing various computer vision tasks. The seminal work by Wang et al. [32] introduced the concept of concatenating images to enable the application of a single model to multiple tasks. Zhang et al. [40] further extended this approach by proposing a prompt retrieval framework to automatically select the most relevant examples for a given query, leading to improved performance. Additionally, integrating multiple example samples into a single grid image has been shown to enhance performance as the number of examples increases [40].

Nevertheless, these approaches have primarily focused on photorealistic images, and their effectiveness in non-photorealistic domains, such as cartoon characters, remains unexplored. Cartoon and pixel-style images, which represent non-photorealistic rendering [3, 16, 17, 33], pose unique challenges due to their distinctive appearance and the difficulty in collecting large-scale datasets [15, 16, 33, 35]. Consequently, generating cartoon-style characters via TTI models often results in frequent visual hallucinations, such as characters with three legs or one arm, as shown in Fig. 2. To address this problem, a dedicated refinement or post-processing step is necessary. However, to the best of our knowledge, no research has been conducted to specifically tackle this issue in cartoon-style images.

To bridge this gap, we present a novel visual hallucination detection system based on pose-aware in-context visual learning (PA-ICVL). Our approach takes inspiration from recent progress in the area of in-context visual learning [32, 40]. However, we extend these methods to address the unique challenges posed by cartoon character images by incorporating numerical pose information along-

*Equal contribution.

†Corresponding author.

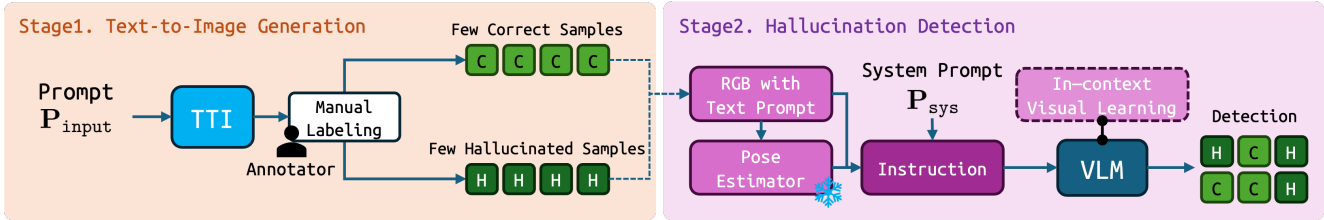


Figure 1. Pipeline of text-to-image generation and hallucination detection.



Figure 2. Examples of visual hallucinations in cartoon/pixel rendering images generated by TTI models. More samples can be found in Appendices A.

side the visual data, necessitating a novel adaptation of the existing techniques. Unlike previous methods, we do not perform additional parameter training on the given input-output pairs. Instead, we propose a repetitive information injection that gradually provides the model with both visual and pose information while maintaining a history of the context. This enables our model to effectively utilize the in-context learning paradigm for the specific task of visual hallucination detection in non-photorealistic domains, allowing VLMs to make more accurate decisions in identifying visual hallucinations.

2. Challenges in Detecting Visual Hallucinations

Before our proposal, we conducted pre-analysis and trials to detect visual hallucinations without the use of VLMs. Initially, we sought to employ image classification by generating a dataset with labels, yet we were confronted with a data imbalance issue due to the unpredictable and uneven generation of hallucination samples from the TTI process. In an effort to mitigate this challenge, we experimented with the deliberate generation of hallucination samples. However, this approach led us to face a gap in appearance between real and fabricated hallucinations. Through these endeavors, we concluded that amassing a large dataset for hallucination samples is not only limited but also a non-trivial task. This realization prompted us to explore the potential of learning from a few samples for the detection of hallucinations.

Further details on our pre-analysis can be found in Appendices C.

3. Methodology

For efficient and highly accurate detection of hallucinations in cartoon character images, a meticulously designed pipeline is required. Fig. 1 illustrates our pipeline. In the text-to-image generation stage, a limited number of images are generated for use in subsequent stages. These images are then analyzed by annotators for application in the PA-ICVL process.

PA-ICVL let VLMs do other tasks without weight update. In our task, VLMs should learn hallucination case with elaborately designed instruction so that it become visual assistant to detect hallucination in second stage. Under cartoon style character generation, visual hallucination are perceptually distinguishable as shown in Fig. 2.

3.1. In-Context Visual Learning for Visual Hallucination

With few hallucination sample pairs, we would like the model to detect whether generated image is correct or hallucinated. To do that, manually curated hallucination N images by annotator is labeled as *Question(User) : Is this image a hallucination sample?*, *Answer(VLM) : Yes/No*. With these prepared samples, VLM $g(\cdot)$ can become an visual assistant for hallucination detection based on PA-ICVL. Specifically, given input prompt \mathbf{P}_{input} (we provide used prompt in Appendices H.), cartoon character image $\mathbf{X}_{unknown}$ is generated as $\mathbf{X}_{unknown} = f(\mathbf{P}_{input})$ where $f(\cdot)$ is a TTI models. Through manual human labeling, our few visual instruction set \mathcal{D}^H is validated as $\mathcal{D}^H = ([\mathbf{X}_{known}^1, \mathbf{T}_*^1, \mathbf{P}_{inst}^1], \dots, [\mathbf{X}_{known}^N, \mathbf{T}_*^N, \mathbf{P}_{inst}^N])$ where N is the number of instruction samples. In PA-ICVL step, general-purpose VLM $g(\cdot)$ first become detector as $\hat{g}(\cdot) = g(\mathbf{P}_{sys})$ where \mathbf{P}_{sys} is system prompt to convert general-purpose VLM to hallucination detector. Then, $\hat{g}(\cdot)$ learn each instruction samples \mathbf{X}_{inst}^t extracted from visual instruction dataset:

$$\mathbf{X}_{inst}^t = [\mathbf{X}_{known}^t, \mathbf{T}_*^t, \mathbf{P}_{inst}^t], (1 \leq t \leq N) \quad (1)$$

where \mathbf{P}_{inst}^t is t -th instruction prompt which includes the reason why this sample is hallucinated/correct, \mathbf{T}_*^t is

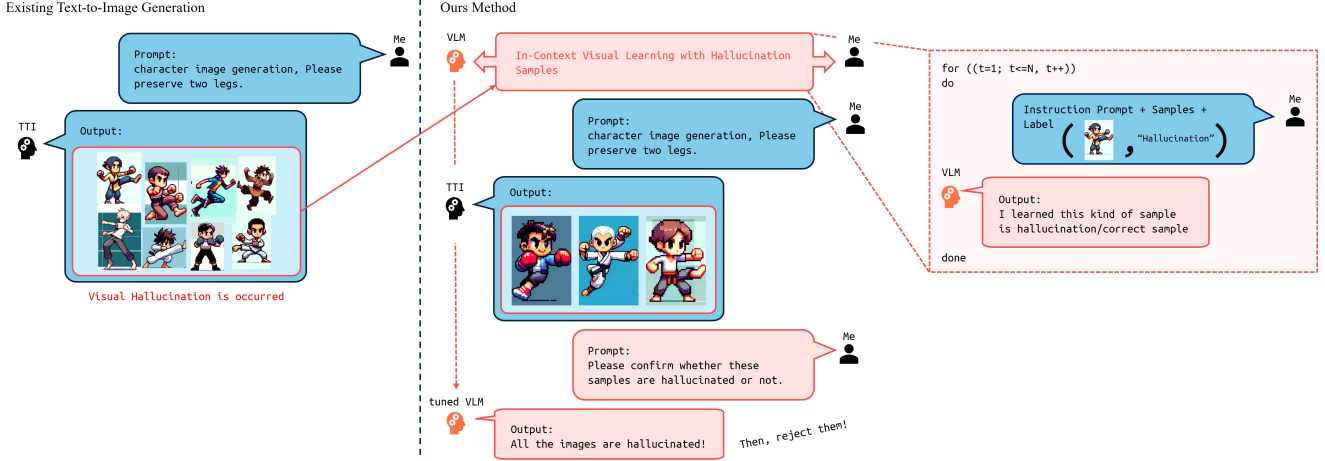


Figure 3. Schematic overview of visual hallucination detection including TTI process.

the t -th label indicating whether or not visual hallucination. Through human manual validation, \mathbf{T}_*^t is obtained as $\mathbf{T}_h =$ "This is hallucinated one" or $\mathbf{T}_c =$ "This is correct one" for hallucination and correct sample respectively.

Algorithm 1 POSE-AWARE IN-CONTEXT VISUAL LEARNING

Input: Hallucination dataset $\mathcal{D}^H = ([\mathbf{X}_{\text{known}}^1, \mathbf{M}_{\text{known}}^1, \mathbf{T}_*^1, \mathbf{P}_{\text{inst}}^1], \dots, [\mathbf{X}_{\text{known}}^N, \mathbf{M}_{\text{known}}^N, \mathbf{T}_*^N, \mathbf{P}_{\text{inst}}^N])$, system prompt \mathbf{P}_{sys} , a general-purpose VLM $g(\cdot)$.

Output: learned VLM $\hat{g}(\cdot)$

- 1: $t \leftarrow 1$
- 2: // initialize VLM
- 3: $\hat{g}_{t-1}(\cdot) \leftarrow g(\mathbf{P}_{\text{sys}})$
- 4: **while** $t \neq N+1$ **do**
- 5: // Allocate sample from dataset (see Eq. 2)
- 6: $\mathbf{X}_{\text{inst}}^t \leftarrow \mathcal{D}^H$
- 7: // In-Context Visual Learning (see Sec. 3.1)
- 8: $\hat{\mathbf{T}}_*^t \leftarrow \hat{g}_{t-1}(\mathbf{X}_{\text{inst}}^t)$
- 9: **if** $\hat{\mathbf{T}}_*^t == \mathbf{T}_*^t$ **then**
- 10: $\hat{g}_t(\cdot) \leftarrow \hat{g}_{t-1}(\cdot)$
- 11: $t \leftarrow t+1$
- 12: **return** $\hat{g}_{t=N}(\cdot)$

3.2. Pose Guidance

In hallucination samples as shown in Fig. 2, we found that almost visual hallucination samples in cartoon domain include body structures issues such as arms, legs or head. Under this observation, we decide to leverage pose estimation results to further improve detection performance of tuned VLM. Given pre-trained pose estimator $\mathcal{E}_\theta(\cdot)$ which has cartoon-domain trained weight θ , pose map \mathbf{M} is extracted as $\mathbf{M}_* = \mathcal{E}_\theta(\mathbf{X}_*)$, where $*$ is known or unknown. Thus, final input of VLM is changed from Eq. 1 to:

$$\mathbf{X}_{\text{inst}}^t = [\mathbf{X}_{\text{known}}^t, \mathbf{M}_{\text{known}}^t, \mathbf{T}_*^t, \mathbf{P}_{\text{inst}}^t], (1 \leq t \leq N), \quad (2)$$

where $\mathbf{M}_{\text{known}}^t$ is t -th pose map from $\mathbf{X}_{\text{known}}^t$. PA-ICVL is outlined in the Alg. 1.

3.3. Visual Hallucination Detection

Given newly generated image $\mathbf{X}_{\text{unknown}}$, pose estimator $\mathcal{E}_\theta(\cdot)$ extract pose map as $\mathbf{M}_{\text{unknown}} = \mathcal{E}_\theta(\mathbf{X}_{\text{unknown}})$. Then, our VLM $\hat{g}(\cdot)$ predict hallucination label $\hat{\mathbf{T}}_p$ as $\hat{\mathbf{T}}_p = \hat{g}(\mathbf{X}_{\text{unknown}}, \mathbf{M}_{\text{unknown}})$. Finally, new generated one $\mathbf{X}_{\text{unknown}}$ is determined as :

$$\mathbf{X}_{\text{unknown}} = \begin{cases} \hat{\mathbf{X}}_{\text{known},c} & \text{if } \hat{\mathbf{T}}_p = \mathbf{T}_c \\ \hat{\mathbf{X}}_{\text{known},h} & \text{if } \hat{\mathbf{T}}_p = \mathbf{T}_h \end{cases} \quad (3)$$

After detecting all the samples in new hallucination-unknown dataset, this dataset $\{\mathbf{X}_{\text{unknown}}\}$ is validated as hallucination-known dataset $\{\hat{\mathbf{X}}_{\text{known},c}\}$, i.e., non-hallucinated samples with different the number of samples. Overview for hallucination detection process is illustrated in Fig. 3.

4. Experiments

For character appearance, we limit the style as cartoon and pixel using prompt as five-head-figure. For TTI model, we adopt DALL-E3¹ [5]. This is because we found that other TTI models (SDv1.5 [29], PixArt- α [9, 10] and so on) cannot generate consistent appearance (see Appendices D for TTI comparison). Final TTI image \mathbf{X} and input size of pose estimation has 384 by 256. For pose estimator fine-tuning, we used COCO [20] format for joint labeling which

¹Note that we found meaningful tendency between ChatGPT platform and pure DALL-E3 API. We invite reader to Appendices E for details.

is represented as 16 joint feature as raw pose map M . For VLMs, GPT-4.0 Vision [1] is used.

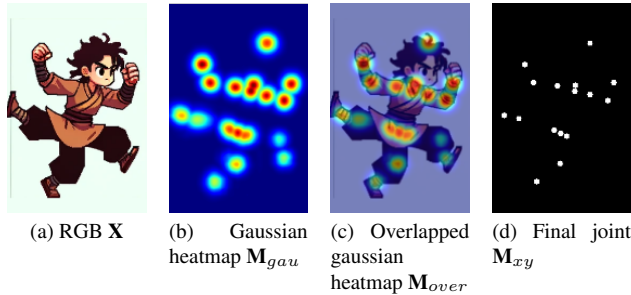


Figure 4. Example of input data about VLM for ablation study.

4.1. Quantitative Evaluation with Ablation

VLM learned our state using the 5 correct and 5 hallucination train samples (total 10 images for PA-ICVL) and detect the test samples using 60 images for each class (total 120 images for evaluation). To quantitatively evaluate the performance, we calculated the number of correct predictions relative to the total number of test samples for each class. This metric provides a clear indication of the learned VLM’s ability to accurately detect visual hallucinations in machine-generated pixel character images.

Model	Task Name	Inputs for VLM
A	System Prompt	
B	A + Hallucination Define.	
C	B + In-Context Learning	\mathbf{X}
D	Pose Guidance	.
D-1	C + Overlapped Heatmap	\mathbf{M}_{over}
D-2	C + Heatmap	$\mathbf{X}, \mathbf{M}_{over}$
D-3	C + Joint (image)	$\mathbf{X}, \mathbf{M}_{xy}$
D-4 [†]	C + Joint (text)	$\mathbf{X}, \text{text}(\mathbf{M}_{xy})$

Table 1. Ablation list. † denotes our final model

To verify the effectiveness of our method, we conduct ablation study as shown in Tab. 1. Model **A** is system prompt only VLMs. Model **B** is system prompt with the definition about hallucination. Model **C** is visual in-context learning. Multiple models **D** are our methods, PA-ICVL with various pose map format as shown in Fig. 4.

As shown in Fig. 5, our quantitative results demonstrate that model **A** seems to detect inputs randomly with about 50% accuracy, while model **B** shows a better score than model **A**, but still performs poorly. In contrast, model **C**, which learned from our hallucination cases, exhibits significantly better detection performance. Building upon this foundation, pose-aware models **D-1**, **D-2**, and **D-3** demonstrate improved performance thanks to the additional pose input. Beyond using the image modality for pose, the language modality-based pose-aware model **D-4** achieves the

best score. We hypothesize that textual joint data can provide more precise posture information, enabling the VLM to effectively compare the input RGB image with the pose data to identify hallucinations.

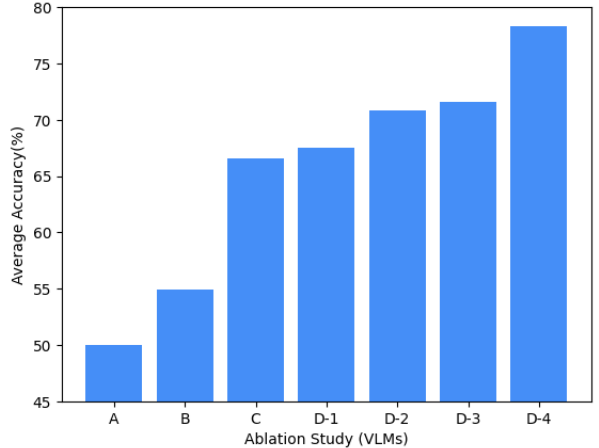


Figure 5. Quantitative evaluation with ablation study.

5. Conclusion

Our research has introduced a novel visual hallucination detection system for cartoon character images generated by large-scale TTI models. Inspired by recent progress in in-context visual learning, we leveraged PA-ICVL, integrating RGB images with pose information from a fine-tuned pose estimator. This method extends existing in-context visual learning strategies by adding numerical pose data to visual inputs, utilizing a distinctive repetitive information injection approach. By iteratively injecting visual and pose data into the model within a contextual history, our system leverages the advantages of in-context learning without needing additional training. As a result, VLMs have become more precise in identifying visual hallucinations. Our experiments have demonstrated that our approach significantly improves upon baseline methods, notably enhancing TTI models by mitigating visual hallucinations and broadening their applicability, particularly in scenarios where visual accuracy is paramount. Specifically, through testing under various pose information conditions, we found that incorporating text-based joint information proved to be the most effective strategy. Future work will aim to integrate additional modalities and adapt our approach to various non-photorealistic styles, enhancing TTI model applications. Our method, addressing cartoon image challenges, establishes new benchmarks in detecting visual hallucinations in such domains.

References

[1] Josh Achiam, Steven Adler, Sandhini Agarwal, Lama Ahmad, Ilge Akkaya, Florencia Leoni Aleman, Diogo Almeida,

- Janko Altmenschmidt, Sam Altman, Shyamal Anadkat, et al. Gpt-4 technical report. *arXiv preprint arXiv:2303.08774*, 2023. 1, 4
- [2] Jean-Baptiste Alayrac, Jeff Donahue, Pauline Luc, Antoine Miech, Iain Barr, Yana Hasson, Karel Lenc, Arthur Mensch, Katherine Millican, Malcolm Reynolds, et al. Flamingo: a visual language model for few-shot learning. *Advances in Neural Information Processing Systems*, 35:23716–23736, 2022. 1
- [3] Jihye Back, Seungkwon Kim, and Namhyuk Ahn. Webtoonme: A data-centric approach for full-body portrait stylization. In *SIGGRAPH Asia 2022 Technical Communications*, pages 1–4. ACM, 2022. 1
- [4] Haoran Bai, Di Kang, Haoxian Zhang, Jinshan Pan, and Linchao Bao. Ffhq-uv: Normalized facial uv-texture dataset for 3d face reconstruction. In *Proceedings of the IEEE/CVF Conference on Computer Vision and Pattern Recognition*, pages 362–371, 2023. 7
- [5] James Betker, Gabriel Goh, Li Jing, Tim Brooks, Jianfeng Wang, Linjie Li, Long Ouyang, Juntang Zhuang, Joyce Lee, Yufei Guo, et al. Improving image generation with better captions. *Computer Science*. <https://cdn.openai.com/papers/dall-e-3.pdf>, 2(3):8, 2023. 3, 7, 8
- [6] Andreas Blattmann, Tim Dockhorn, Sumith Kulal, Daniel Mendelevitch, Maciej Kilian, Dominik Lorenz, Yam Levi, Zion English, Vikram Voleti, Adam Letts, et al. Stable video diffusion: Scaling latent video diffusion models to large datasets. *arXiv preprint arXiv:2311.15127*, 2023. 1
- [7] Sanghyun Byun, Bumsoo Kim, Wonseop Shin, Yonghoon Jung, and Sanghyun Seo. Transfer learning based parameterized 3d mesh deformation with 2d stylized cartoon character. *KSH Transactions on Internet & Information Systems*, 17(11), 2023. 9
- [8] Z. Cao, G. Hidalgo Martinez, T. Simon, S. Wei, and Y. A. Sheikh. Openpose: Realtime multi-person 2d pose estimation using part affinity fields. *IEEE Transactions on Pattern Analysis and Machine Intelligence*, 2019. 8
- [9] Junsong Chen, Yue Wu, Simian Luo, Enze Xie, Sayak Paul, Ping Luo, Hang Zhao, and Zhenguo Li. Pixart- δ : Fast and controllable image generation with latent consistency models, 2024. 3
- [10] Junsong Chen, Jincheng Yu, Chongjian Ge, Lewei Yao, Enze Xie, Yue Wu, Zhongdao Wang, James Kwok, Ping Luo, Huchuan Lu, and Zhenguo Li. Pixart- α : Fast training of diffusion transformer for photorealistic text-to-image synthesis, 2023. 3, 8
- [11] Haodong Duan, Kwan-Yee Lin, Sheng Jin, Wentao Liu, Chen Qian, and Wanli Ouyang. Trb: a novel triplet representation for understanding 2d human body. In *Proceedings of the IEEE/CVF international conference on computer vision*, pages 9479–9488, 2019. 9
- [12] Or Hirschorn and Shai Avidan. Pose anything: A graph-based approach for category-agnostic pose estimation. *arXiv preprint arXiv:2311.17891*, 2023. 8
- [13] Xiaowei Hu, Zhe Gan, Jianfeng Wang, Zhengyuan Yang, Zicheng Liu, Yumao Lu, and Lijuan Wang. Scaling up vision-language pre-training for image captioning. In *Proceedings of the IEEE/CVF conference on computer vision and pattern recognition*, pages 17980–17989, 2022. 1
- [14] Lei Huang, Weijiang Yu, Weitao Ma, Weihong Zhong, Zhangyin Feng, Haotian Wang, Qianglong Chen, Weihua Peng, Xiaocheng Feng, Bing Qin, et al. A survey on hallucination in large language models: Principles, taxonomy, challenges, and open questions. *arXiv preprint arXiv:2311.05232*, 2023. 1
- [15] Bumsoo Kim, Sanghyun Byun, Yonghoon Jung, Wonseop Shin, Sareer UI Amin, and Sanghyun Seo. Minecraftify: Minecraft style image generation with text-guided image editing for in-game application. *arXiv preprint arXiv:2402.05448*, 2024. 1
- [16] Bumsoo Kim, Abdul Muqet, Kyuchul Lee, and Sanghyun Seo. Toonaging: Face re-aging upon artistic portrait style transfer. *arXiv preprint arXiv:2402.02733*, 2024. 1
- [17] Seungkwon Kim, Chaeheon Gwak, Dohyun Kim, Kwangho Lee, Jihye Back, Namhyuk Ahn, and Daesik Kim. Cross-domain style mixing for face cartoonization. *arXiv preprint arXiv:2205.12450*, 2022. 1
- [18] Donghoon Lee, Jiseob Kim, Jisu Choi, Jongmin Kim, Minwoo Byeon, Woonhyuk Baek, and Saehoon Kim. Karlo-v1.0.alpha on coyo-100m and cc15m. <https://github.com/kakaobrain/karlo>, 2022. 7, 8
- [19] Yifan Li, Yifan Du, Kun Zhou, Jinpeng Wang, Wayne Xin Zhao, and Ji-Rong Wen. Evaluating object hallucination in large vision-language models. *arXiv preprint arXiv:2305.10355*, 2023. 1
- [20] Tsung-Yi Lin, Michael Maire, Serge Belongie, Lubomir Bourdev, Ross Girshick, James Hays, Pietro Perona, Deva Ramanan, C. Lawrence Zitnick, and Piotr Dollár. Microsoft coco: Common objects in context, 2015. 3
- [21] Haotian Liu, Chunyuan Li, Qingyang Wu, and Yong Jae Lee. Visual instruction tuning. *Advances in neural information processing systems*, 36, 2024. 1
- [22] Simian Luo, Yiqin Tan, Longbo Huang, Jian Li, and Hang Zhao. Latent consistency models: Synthesizing high-resolution images with few-step inference, 2023. 7, 8
- [23] Simian Luo, Yiqin Tan, Suraj Patil, Daniel Gu, Patrick von Platen, Apolinário Passos, Longbo Huang, Jian Li, and Hang Zhao. Lcm-lora: A universal stable-diffusion acceleration module. *arXiv preprint arXiv:2311.05556*, 2023. 8
- [24] MMPose Contributors. OpenMMLab Pose Estimation Toolbox and Benchmark. <https://github.com/open-mmlab/mmpose>, Aug. 2020. License: Apache-2.0. 9
- [25] Abdul Muqet, Kyuchul Lee, Bumsoo Kim, Yohan Hong, Hyungrae Lee, Woonggon Kim, and KwangHee Lee. Video face re-aging: Toward temporally consistent face re-aging. *arXiv preprint arXiv:2311.11642*, 2023. 7
- [26] Alex Nichol, Prafulla Dhariwal, Aditya Ramesh, Pranav Shyam, Pamela Mishkin, Bob McGrew, Ilya Sutskever, and Mark Chen. Glide: Towards photorealistic image generation and editing with text-guided diffusion models. *arXiv preprint arXiv:2112.10741*, 2021. 1
- [27] Dustin Podell, Zion English, Kyle Lacey, Andreas Blattmann, Tim Dockhorn, Jonas Müller, Joe Penna, and

- Robin Rombach. Sdxl: Improving latent diffusion models for high-resolution image synthesis. *arXiv preprint arXiv:2307.01952*, 2023. 1, 7, 8
- [28] Aditya Ramesh, Mikhail Pavlov, Gabriel Goh, Scott Gray, Chelsea Voss, Alec Radford, Mark Chen, and Ilya Sutskever. Zero-shot text-to-image generation. In *International Conference on Machine Learning*, pages 8821–8831. PMLR, 2021. 1
- [29] Robin Rombach, Andreas Blattmann, Dominik Lorenz, Patrick Esser, and Björn Ommer. High-resolution image synthesis with latent diffusion models. In *Proceedings of the IEEE/CVF conference on computer vision and pattern recognition*, pages 10684–10695, 2022. 1, 3
- [30] Ke Sun, Bin Xiao, Dong Liu, and Jingdong Wang. Deep high-resolution representation learning for human pose estimation. In *Proceedings of the IEEE/CVF conference on computer vision and pattern recognition*, pages 5693–5703, 2019. 9
- [31] Hugo Touvron, Thibaut Lavril, Gautier Izacard, Xavier Martinet, Marie-Anne Lachaux, Timothée Lacroix, Baptiste Rozière, Naman Goyal, Eric Hambro, Faisal Azhar, et al. Llama: Open and efficient foundation language models. *arXiv preprint arXiv:2302.13971*, 2023. 1
- [32] Xinlong Wang, Wen Wang, Yue Cao, Chunhua Shen, and Tiejun Huang. Images speak in images: A generalist painter for in-context visual learning. In *Proceedings of the IEEE/CVF Conference on Computer Vision and Pattern Recognition*, pages 6830–6839, 2023. 1
- [33] Zongwei Wu, Liangyu Chai, Nanxuan Zhao, Bailin Deng, Yongtuo Liu, Qiang Wen, Junle Wang, and Shengfeng He. Make your own sprites: Aliasing-aware and cell-controllable pixelization. *ACM Transactions on Graphics (TOG)*, 41(6):1–16, 2022. 1
- [34] Ziwei Xu, Sanjay Jain, and Mohan Kankanhalli. Hallucination is inevitable: An innate limitation of large language models. *arXiv preprint arXiv:2401.11817*, 2024. 1
- [35] Shuai Yang, Liming Jiang, Ziwei Liu, and Chen Change Loy. Pastiche master: Exemplar-based high-resolution portrait style transfer. In *Proceedings of the IEEE/CVF Conference on Computer Vision and Pattern Recognition*, pages 7693–7702, 2022. 1
- [36] Yi Yang and Deva Ramanan. Articulated pose estimation with flexible mixtures-of-parts. In *CVPR 2011*, pages 1385–1392. IEEE, 2011. 9
- [37] Chi Zhang, Yiwen Chen, Yijun Fu, Zhenglin Zhou, Gang Yu, Billzb Wang, Bin Fu, Tao Chen, Guosheng Lin, and Chunhua Shen. Styleavatar3d: Leveraging image-text diffusion models for high-fidelity 3d avatar generation. *arXiv preprint arXiv:2305.19012*, 2023. 1
- [38] Jingyi Zhang, Jiaying Huang, Sheng Jin, and Shijian Lu. Vision-language models for vision tasks: A survey. *arXiv preprint arXiv:2304.00685*, 2023. 1
- [39] Lvmin Zhang, Anyi Rao, and Maneesh Agrawala. Adding conditional control to text-to-image diffusion models. In *Proceedings of the IEEE/CVF International Conference on Computer Vision*, pages 3836–3847, 2023. 1
- [40] Yuanhan Zhang, Kaiyang Zhou, and Ziwei Liu. What makes good examples for visual in-context learning? *Advances in Neural Information Processing Systems*, 36, 2024. 1
- [41] Wayne Xin Zhao, Kun Zhou, Junyi Li, Tianyi Tang, Xiaolei Wang, Yupeng Hou, Yingqian Min, Beichen Zhang, Junjie Zhang, Zican Dong, et al. A survey of large language models. *arXiv preprint arXiv:2303.18223*, 2023. 1
- [42] Lianmin Zheng, Wei-Lin Chiang, Ying Sheng, Siyuan Zhuang, Zhonghao Wu, Yonghao Zhuang, Zi Lin, Zhuohan Li, Dacheng Li, Eric Xing, et al. Judging llm-as-a-judge with mt-bench and chatbot arena. *Advances in Neural Information Processing Systems*, 36, 2024. 9

Appendices

A. Visual Hallucination in Cartoon Domain

Cartoon domain has unique appearance. The cases and level of visual hallucination are quite different from realistic domain. When we generate many cartoon image from TTI, we found that there are two classes about hallucination tendency as shown in Fig. 6: one is uncompleted whole-body having one arm, one leg or even no head as shown in Fig. 6a, other one is over-depiction of body components such as three arms, three legs as shown in Fig. 6b. These hallucination types led us utilize pose estimation for visual hallucination detection in cartoon image.

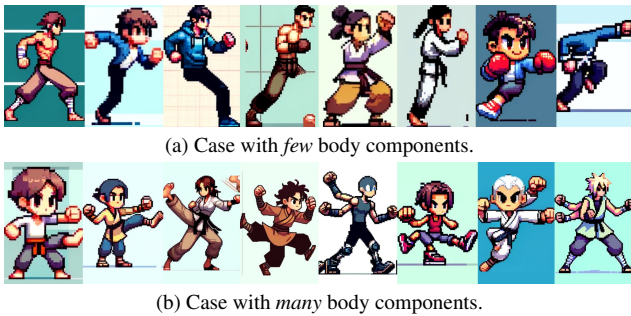


Figure 6. Hallucination classes in cartoon domain.

B. Visual Hallucination in Realistic Domain

Realistic domain is in contrast to cartoon domain. Since realistic domain has relatively more curated dataset, it is not easy to find large defects in generated image. Nonetheless, there are still fine defects such as impossible hand joints as shown in Fig. 7 or six fingers as shown in Fig. 8. Here, we used popular machine-generated samples to show the cases of visual hallucination in realistic domain.

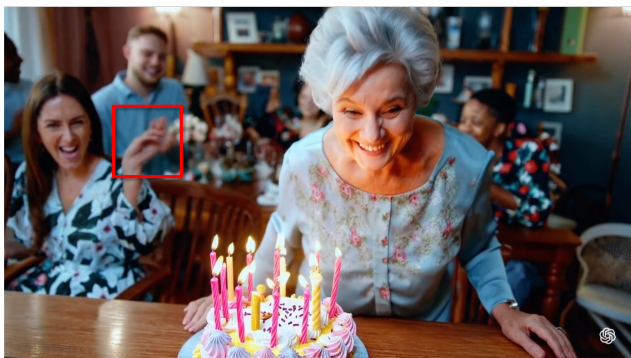


Figure 7. Example of hallucination in SORA. In this demo video we can see an impossible articulated hand at about 8 seconds in.

²https://www.reddit.com/r/StableDiffusion/comments/15wvdd0/sdxl_is_a_lot_better_but_still/

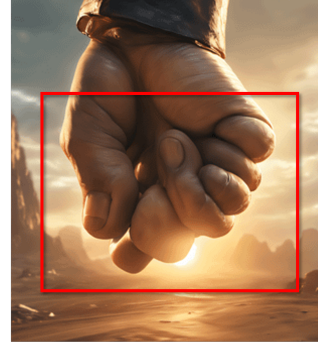


Figure 8. Example of visual hallucination in SDXL [27] output².

C. Challenges in Detecting Visual Hallucinations

We would like to provide some insights and limitations through our pre-analysis and trials to detect visual hallucination without VLMs.

C.1. Class Imbalance Problem

Our first approach was to adopt image classification to detect it by generating hallucination dataset with label. To do that, we wanted to gather correct (*i.e.*, non-hallucination) and hallucination samples through multiple TTI process. However we encountered data imbalance problem due to the fact that hallucination sample is unpredictably and unevenly generated with few samples from all the output according to textual prompts. Empirically, we faced about 10 hallucination samples per 100 images, but it is quite different according to input prompt and settings.

C.2. Deliberated Hallucination Generation

To address aforementioned class imbalance issue, we wanted to generate dataset for hallucination samples deliberately such as [4, 25], but faced appearance gap problem between real and fake hallucination as depicted in Fig. 9. We found that deliberately generated samples through our hallucination prompt has exaggerated structure (Fig. 9b.) much far ways from real hallucination (Fig. 9a). Thus, we concluded that gathering large dataset for hallucination samples is limited and non-trivial, and it makes us use few-samples for hallucination detection.

D. Cartoon Rendering Comparison with Various Large Text-to-Image Models

We evaluate TTI models which include DALL-E3 [5], SDv2.1³ [22], SDXLv1.0⁴ [27], Karlo⁵ [18], PIXART- α ⁶

³<https://huggingface.co/spaces/stabilityai/stable-diffusion>

⁴<https://huggingface.co/stabilityai/stable-diffusion-xl-base-1.0>

⁵<https://karlo.ai/>

⁶<https://huggingface.co/spaces/PixArt-alpha/PixArt-alpha>



Figure 9. Comparison between real hallucination samples from normal prompt and fake hallucination samples from deliberately designed hallucination prompt.



Figure 10. Comparison for cartoon rendering quality with SOTA TTI models

[10], PIXART- α with LCM⁷. For comparison in terms of cartoon rendering quality, we used same input prompt for every TTI models. For Karlo, the input prompts we used were also converted to combinations of words because, in Karlo website, we found that user typically used word format rather than sentences.

As shown in Fig. 10, we found that all the models generate non-plausible appearance for cartoon-pixel character except DALL-E3. Due to that, we used DALL-E3 for our TTI model.

⁷<https://huggingface.co/spaces/PixArt-alpha/PixArt-LCM>

E. ChatGPT-4 Vision vs DALL-E3 API

We found that there are some gaps about appearance tendency between ChatGPT-4 Vision through ChatGPT site⁸ and pure DALL-E3 API⁹. We conducted experiments by feeding the TTI prompts into both ChatGPT-4 Vision and the DALL-E3 API to generate images. Empirically, we observed that ChatGPT-4 Vision created images that were closer to our desired output with clean apparent structure compared to DALL-E3 API. We conjecture that this result is derived from ChatGPT’s capability to refine and analyze the provided prompt, which in turn elevates its comprehension of the prompt, leading to the production of superior images.

F. Pose Estimator

Here, we provide some details for our pose estimator including fine-tuning scheme and comparison on other off-the-shelf pose estimators.

F.1. Comparison on Various Pose Estimators

To use visually precise pose joint about cartoon character to VLM, we used our fine-tuned pose estimator (see Appendices F.2 for details of fine-tuning). Here, we show the pose estimation performance with off-the-shelf pose estimators which include PoseAnything [12], OpenPose [8]. For PoseAnything, we used 1-Shot split-1 small model from official repository¹⁰. For OpenPose, we used pose_iter_160000.caffemodel for MPII format from official repository¹¹.

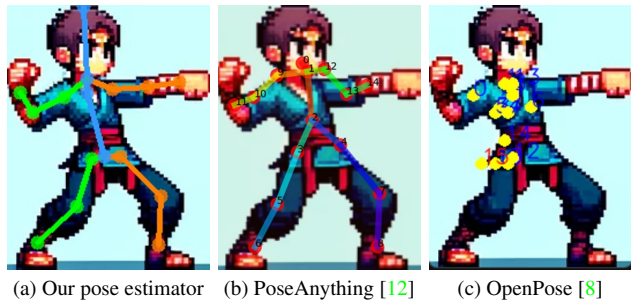


Figure 11. Comparison of pose estimation.

As shown in Fig. 11, we found that there is no one which can predict perceptually plausible joint. This is conjectured that cartoon domain distributed far away from pre-trained weights, leading requirement of fine-tuning with this domain.

⁸<https://openai.com/gpt-4>

⁹<https://openai.com/dall-e-3>

¹⁰<https://github.com/orhir/PoseAnything>

¹¹<https://github.com/CMU-Perceptual-Computing-Lab/openpose>

F.2. Fine-tuning

We fine-tune the pose estimator based on HRNet-w48 [30] (Top-down approach) upon MMPose library [24] with collected 3D cartoon dataset as shown in Fig. 12. Our training scheme is based on [7]. For pose estimation settings, we used MPII-TRB [11] keypoint format (16 joint for whole-body) with inference image size as 384 by 256 using boundary padding. Including 2D illustration and rendered 2D images from 3D model shape, totalling 2400 images in animation, illustration and cartoon domains are used for fine-tuning for about 16K iterations with 32 batch size, achieving 0.8902 PCKh (Percentage of Correct Key-points head) [36] at threshold 0.5.

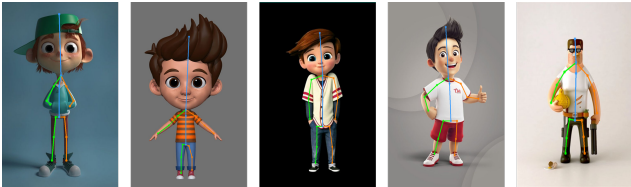


Figure 12. Example of training dataset for pose estimation fine-tuning.

G. Limitations

Our domain, cartoon style character, has extremely wide appearance. Moreover, some cases include ambiguous appearance even in human perception. Therefore, our learned VLM can not detect all the images of wide-range cartoon domain. Additionally, it is known that TTI models and VLMs tend to generate output sensitively with word position-bias, verbosity-bias, self-enhancement-bias [42]. Due to that, it is noteworthy that output or results can be showed as different tendency according to the input data. Through above mentioned things, we would like to mention that there are some limitations to leverage our scheme toward more generalized task directly.

H. Used prompts

H.1. TTI Input prompt list

1. Please design a 2D motion frame pixel style character with a size of 256x384 pixels. Each action should be displayed on a separate row, with the first row being a {kicking, punching, jumping, running, walking .. etc} action (composed of 5 frames) and the second row being a {kicking, punching, jumping, running, walking .. etc} action (composed of 5 frames) that appears to be smoothly connected. The generated actions should not overlap, and the character's color should be simple. The entire sprite sheet should be 1792x1024 in size.

2. Please design a 2D pixel style character with a size of 256x384 pixels. Each action should be displayed on a separate row, with the first row being a {kicking, punching, jumping, running, walking .. etc} action (composed of 5 frames) and the second row being a {kicking, punching, jumping, running, walking .. etc} action (composed of 5 frames) that appears to be smoothly connected. The entire sprite sheet should be 1792x1024 in size.

3. Please design a 2D motion frame pixel style character. Each action should be displayed on a separate row, with the first row being a low-kick action and the second row being a punch action that appears to be smoothly connected. The generated actions should not overlap, and the character's color should be simple. The entire sprite sheet should be 1792x1024 in size.

H.2. Instruction prompt list

System Prompt & Hallucination Definition : You are a hallucination detector, and your mission is to detect if the image has hallucinations. Here I define hallucination as when a character is missing an arm, leg, or has an abnormal number of them (three legs, three arms .. etc). So you need to detect the hallucination I defined in the image and visually describe the hallucination. So as a sample of how to detect this well, we'll provide the following prompts with a hallucination image, a normal image {and joint image, joint file, heatmap image}.

1. **(Model C)** Using RGB image - Correct class : This character is performing a {kicking, punching, jumping, running, walking .. etc} motion with an image of a correct human body with two arms and two legs. This image of a correct human anatomy will be classified as C (correct class) in the future. Your task is to recognize images with correct human anatomy as C images.

2. **(Model C)** Using RGB image - Hallucination class : This character is performing a {kicking, punching, jumping, running, walking .. etc} motion with an abnormal character with {three legs, three arms, no head, no arms, no legs, only one arm, only one leg}. This image of abnormal human anatomy will be classified as H (hallucination class) in the future. Your task is to recognize images with abnormal human anatomy as H images.

3. **(Model D-1)** Using Overlapped heatmap image - Correct class : This image is a pose heatmap obtained from the pose estimator. This character is performing a {kicking, punching, jumping, running, walking .. etc} motion with an image of a correct human body with two arms and two legs. This image of a correct human anatomy will be classified as C (correct class) in the future. Your task is to recognize images with correct human anatomy as C images.

4. **(Model D-1)** Using Overlapped heatmap image - Hallucination class : This image is a pose heatmap obtained from the pose estimator. This character is performing a {kicking, punching, jumping, running, walking .. etc} with {three legs, three arms, no head, no arms, no legs, only one arm, only one leg}. This image of abnormal human anatomy will be classified as H (hallucination class) in the future. Your task is to recognize images with abnormal human anatomy as H images.

5. **(Model D-2)** Using RGB & overlapped heatmap image - Correct class : The first image is an RGB image of the character and the second image is a heatmap of the character's pose using the pose estimator. This character is performing a {kicking, punching, jumping, running, walking .. etc} motion with an image of a normal human body with two arms and two legs. This image of a normal human anatomy will be classified as C (correct class) in the future. Your task is to recognize images with normal human anatomy as C images.

6. **(Model D-2)** Using RGB & overlapped heatmap image - Hallucination class : The first image is an RGB image of the character and the second image is a heatmap of the character's pose using the pose estimator. This character is performing

a {kicking, punching, jumping, running, walking .. etc} motion with {three legs, three arms, no head, no arms, no legs, only one arm, only one leg}. This image of abnormal human anatomy will be classified as H (hallucination class) in the future. Your task is to recognize images with abnormal human anatomy as H images.

7. **(Model D-3)** Using RGB image & Joint (image) - Correct class : The first image is an RGB image of the character and the second image is a keypoint of the character's pose using the pose estimator. This character is performing a {kicking, punching, jumping, running, walking .. etc} motion with an image of a correct human body with two arms and two legs. This image of a correct human anatomy will be classified as C (correct class) in the future. Your task is to recognize images with correct human anatomy as C images.

8. **(Model D-3)** Using RGB image & Joint (image) - Hallucination class : The first image is an RGB image of the character and the second image is a keypoint of the character's pose using the pose estimator. This character is performing a {kicking, punching, jumping, running, walking .. etc} motion with an abnormal character with {three legs, three arms, no head, no arms, no legs, only one arm, only one leg}. This image of abnormal human anatomy will be classified as H (hallucination class) in the future. Your task is to recognize images with abnormal human anatomy as H images.

9. **(Model D-4)** Using RGB image & Joint (text) - Correct class : The first image is an RGB image of the character and the second file is a keypoint of the character's pose using the pose estimator. This character is performing a {kicking, punching, jumping, running, walking .. etc} motion with an image of a correct human body with two arms and two legs. This image of a correct human anatomy will be classified as C (correct class) in the future. Your task is to recognize images with correct human anatomy as C images.

10. **(Model D-4)** Using RGB image & Joint (text) - Hallucination class : The first image is an RGB image of the character and the second file is a keypoint of the character's pose using the pose estimator. This character is performing a {kicking, punching, jumping, running, walking .. etc} motion with an abnormal character with {three legs, three arms, no head, no arms, no legs, only one arm, only one leg}. This image of abnormal human anatomy will be classified as H (hallucination class) in the future. Your task is to recognize images with abnormal human anatomy as H images.